






ARTICLE



<https://doi.org/10.1057/s41599-024-02881-1>

OPEN

Investigating neighborhood adaptability using mobility networks: a case study of the COVID-19 pandemic

Hasan Alp Boz^{1,5}[✉], Mohsen Bahrami^{2,5}[✉], Selim Balcisoy¹, Burcin Bozkaya³, Nina Mazar⁴[✉], Aaron Nichols⁴ & Alex Pentland²

What predicts a neighborhood's adaptability to essential public health policies and shelter-in-place regulations that prevent the harmful spread of COVID-19? To answer this question, we present a novel application of human mobility patterns and human behavior in a network setting. We analyze 2 years of mobility data (January 2019 to December 2020) from New York City and construct weekly mobility networks between census block groups based on aggregated point-of-interest visit patterns. Our results indicate that neighborhoods' socio-economic and geographic characteristics play a significant role in predicting their adaptability to active shelter-in-place policies. Our simulation outcomes reveal that, alongside factors such as race, education, and income, the geographical attributes of neighborhoods, such as access to amenities that satisfy community needs are equally important factors in predicting neighborhood adaptability to public health policies. These findings offer valuable insights that can enhance urban planning strategies, thereby aiding pandemic mitigation efforts and fostering increased adaptability of urban areas in the face of exogenous shocks like the COVID-19 pandemic.

¹Faculty of Engineering and Natural Sciences, Sabanci University, Istanbul 34956, Turkey. ²Massachusetts Institute of Technology, Institute for Data, Systems, and Society, Cambridge, MA 02139, USA. ³Sabanci Business School, Sabanci University, Istanbul 34956, Turkey. ⁴Boston University, Questrom School of Business, Boston, MA 02215, USA. ⁵These authors contributed equally: Hasan Alp Boz, Mohsen Bahrami. ✉email: bozhasan@sabanciuniv.edu; bahrami@mit.edu

Introduction

Mobility in urban and metropolitan settings is the result of the dynamic interaction, over space and time, of a large number of agents with diverse goals and characteristics. Understanding mobility patterns is crucial for predicting future social and economic well-being as well as growth (Chong et al. 2020, Singh et al. 2015).

Studies have established its correlation with social interactions (Bettencourt, 2013, Buera & Oberfield, 2020), health (Garcia-Bulle et al. 2022, Horn et al. 2021), productivity (Bahrami et al. 2023, Bettencourt et al. 2007, Sveikauskas, 1975), and the economic prosperity and resilience of a region (Alvarez et al. 2013, Pan et al. 2013, Schläpfer et al. 2021, Steele et al. 2017, Yabe et al. 2023).

The dynamic interactions in mobility data are complex and are typically represented in a network setting that is able to produce critically important insights (Lazer et al. 2009). Researchers have utilized mobility networks to explore and investigate the effects of the COVID-19 pandemic from various perspectives (Chang et al. 2021, Gauvin et al. 2021, Kraemer et al. 2020, Schlosser et al. 2020). For instance, Schlosser et al. (2020) construct inter-county mobility networks from mobile phone data and display the topological changes as a result of the undertaken non-pharmaceutical interventions (NPI) aimed at reducing the spread of the Coronavirus (Flaxman et al. 2020, Kraemer et al. 2020).

Given the close link between changes in mobility patterns and economic consequences, it is critical for researchers to carefully investigate how diverse environmental and demographic factors have shaped the adaptability of mobility networks to the enforced NPIs during the COVID-19 pandemic. Adaptability, within the framework of this study, is defined as a neighborhood's ability to conform and modify its behavior in response to the constraints imposed by NPIs.

Using network science methodologies, this research aims to enhance the comprehension of scientists and policy-makers regarding the factors that contribute to adaptability in the wake of exogenous shocks. In particular, we expand upon previous research on the impact of the COVID-19 pandemic on human behavior, by examining the alterations in mobility patterns. We use a dynamic network analysis approach, focusing on one of the most important economic hubs in the world: New York City (NYC).

We construct weekly mobility networks spanning from January 2019 to December 2020, in which the nodes represent neighborhoods (i.e., census block groups or CBGs), while the edges between them correspond to the visitors from the source neighborhood to various points-of-interest (POIs) such as restaurants or supermarkets in the target neighborhood.

For every neighborhood within the weekly networks, we compute node and ego-network-based features (Berlingerio et al. 2012) so the resulting feature vectors not only capture the dynamics of local mobility but also encapsulate the relationship with the neighboring CBGs. Such an approach, enables us to incorporate the nuanced complexity of human mobility into our analyses. We investigate the dissimilarity of the resulting feature vectors for each neighborhood, between the same weeks of 2019 and 2020, and break down the results by different socioeconomic groups. Combining the mobility network metrics with data from various sources (e.g., census data and COVID-19 test results), we are able to reveal how disparities in NYC neighborhood characteristics predict dynamic structural changes in mobility networks and behavior.

Network analysis approaches, as demonstrated by a large body of the literature (Aleta et al. 2020, Chang et al. 2021, 2023, Edsberg Møllgaard et al. 2022, Fan et al. 2021, Galeazzi et al. 2021,

Yuan et al. 2023), enable researchers to explore the multifaceted impact of policy changes on mobility outcomes. Mobility networks coupled with epidemiological models are employed in different settings such as evaluating the effect of business closures on case counts (Chang et al. 2021) and designing optimal vaccine distribution policies (Yuan et al. 2023). Furthermore, network analyses serve as valuable tools for elucidating latent mobility patterns during the pandemic. Møllgaard et al. Edsberg Møllgaard et al. (2022) investigate how different travel behaviors play a part during the pandemic by applying factorization techniques on mobility networks.

In contrast to existing studies, our aim is to dissect the topological changes within the mobility networks over the course of the pandemic using established network metrics, such as centrality indicators. This approach enables us to rapidly discern and analyze the altering landscape of interactions and connections within these networks, providing valuable insights into urban adaptability in the face of a public health crisis. For example, an exploration of the *betweenness* centrality metric can uncover the specific role played by certain neighborhoods during the pandemic. This may involve acting as a crucial bridge among various neighborhoods (nodes) in a mobility network, consequently generating a spreader effect.

Additionally, we utilize a straightforward yet widely acknowledged framework rooted in the well-established Huff gravity model (Huff, 1964) to simulate the mobility flows among neighborhoods (i.e., CBGs). This approach enables us to model and simulate diverse hypothetical scenarios by adjusting POI densities, facilitating analyses of both mobility patterns and adaptability. The simplicity of this framework eliminates the necessity for intricate settings or complex configurations.

The results of our study indicate that the centrality metrics and geographic attributes significantly predict neighborhood adaptability to shelter-in-place orders. In addition to confirming the results of previous research (Althouse et al. 2020, Chang et al. 2021, Chetty et al. 2020, Heroy et al. 2021, Hunter et al. 2021), our findings reveal that not only are race, education, and income important factors in predicting neighborhood adaptability to shelter-in-place orders but so are geographical attributes such as access to diverse amenities that satisfy community needs. This indicates that in the same city, communities with similar socioeconomic and demographic features may have different mobility responses based on their neighborhoods' urban structure.

Using the information extracted from the mobility network structure, we study the case of the COVID-19 hotspots to investigate which neighborhoods act as the COVID-19 bridges among the hotspots and other neighborhoods and uncover the associated factors. We then utilize the Huff gravity model to analyze how higher levels of access to essential businesses (e.g., grocery stores) could potentially reduce the interaction among the COVID-19 hotspots and other neighborhoods, leading to a reduction in infection rates and saving more lives. The findings of this study offer significant insights and suggest policies aimed at improving urban planning strategies. Implementing these recommendations can strengthen efforts to alleviate the impact of pandemics, ultimately enhancing the resilience of urban areas to external shocks like the COVID-19 pandemic, which significantly affects and constrains movements and interactions.

Methods

Datasets

SafeGraph mobility and places data. The dataset released by *SafeGraph* (www.safegraph.com) provides fine-grained user geolocation information collected through the smartphone

applications of millions of users who consented to share their live location. The data is anonymized and then aggregated by the total visits from CBGs to POIs of various categories (e.g., restaurants, grocery stores, and supermarkets) within a defined time period (i.e., weekly and monthly). More specifically, we use the *Weekly Patterns*(SafeGraph) dataset that provides the weekly aggregated visits from January 2019 to December 2020. The patterns dataset is geographically filtered with respect to the administrative boundaries of the New York Metropolitan Area, encompassing 6,493 CBGs from New York City, and 333,241 POIs in total.

Google COVID-19 community mobility reports. This dataset is prepared by Google to provide insights into mobility trends in order to help understand communities' responses to interventions against the COVID-19 pandemic. The data is collected from various smartphone applications including Google Maps. The data shows the dynamics of mobility trends by region, across different POI categories compared to a baseline day that represents a normal day prior to the pandemic. The baseline is the median value from the 5-week period from January 3rd to February 6th, 2020. The POI categories include retail and recreation, groceries and pharmacies, parks, transit stations, workplaces, and residential buildings.

COVID-19 cases and infection rates. The Center for Systems Science and Engineering (CSSE) at Johns Hopkins University (Badr et al. 2023) provides a COVID-19 data catalog presenting the latest updates all around the world with differing granularity levels. In NYC, the statistics for variables such as new cases, test counts, and deaths, are provided by ZIP Code Tabulation Areas (ZCTAs). A CBG may be located inside the borders of multiple ZCTAs. In order to work with the estimated weekly cases per CBG, the numbers were inferred by taking a weighted average based on the ratio of the population of a CBG in each ZCTA and its corresponding COVID-19 case rate. Assume S is the set of ZCTAs that geographically intersect with CBG_i . Then the number of COVID-19 cases for CBG_i at time t are estimated using the following equations.

$$w_{ij} = \frac{\text{population of } CBG_i \text{ in } ZCTA_j}{\text{population of } ZCTA_j} \quad (1)$$

$$CCBG_i^t = \sum_{j \in S} (w_{ij} \times case_j^t) \quad (2)$$

$CCBG_i^t$ denotes the estimated COVID-19 cases in CBG_i at time t , and $case_j^t$ is the number of COVID cases in $ZCTA_j$ at time t . Furthermore, the resulting case counts are normalized by the number of residents in each CBG to obtain a more accurate estimate of infection rates.

The United States Census data. The American Community Survey (ACS) of the U.S. Census Bureau reports the estimates of demographic features at a CBG level. The most recently published 5 year ACS data collected in 2019, is utilized to extract the demographic features, namely: total population, median household income, education level, commuting time, and population distribution by race for each CBG. The resulting features are also represented with corresponding percentile levels.

New York metropolitan area. In 2019, New York Metropolitan Area hosted the highest population at 19.22 million as one of the leading economies in the U.S. with 1.522 Billion Dollars (Statista). The metropolitan area consists of counties from four different states, New York, New Jersey, Connecticut, and Pennsylvania. In total, 7,809 census tracts and 23 counties are represented. POIs provided by the SafeGraph Patterns dataset are filtered by their

location with respect to the New York Metropolitan area. New York City (NYC) with about 9 million residents is the largest city in the New York Metropolitan area containing 6,493 CBGs. NYC is also divided into five administrative boundaries called boroughs. Those five boroughs are Manhattan, Brooklyn, Bronx, Queens, and Staten Island.

Mobility networks. We model the mobility patterns among CBGs as weighted directed networks, $G^{(t)} = (V^{(t)}, E^{(t)})$, for each time step t . In this context, the nodes $V^{(t)}$ correspond to CBGs, and the edges $E^{(t)}$ depict the visits from the source CBG i to the target CBG j , with the number of visits recorded as the edge weight $w_{ij}^{(t)}$. The time steps span from January 2019 to December 2020, each representing a week. The Weekly Patterns dataset provides weekly aggregated number of visits from CBGs to POIs. To construct the mobility networks of CBGs, we exploit the home CBG information of a POI. The number of visits between CBGs i and j is obtained by the aggregation of all visits made by the residents of CBG i to all of the POIs inside CBG j in a time step. For further details on network construction, please see the Supplementary Information.

Temporal topological shifts. To showcase how the mobility network structure evolves over time, we begin by examining the dissimilarities between paired weekly networks from 2019 and 2020. We then further break down the nodes based on demographic groups. Subsequently, we explore the connection between centrality metrics and these demographic groups.

Dissimilarity analysis. To quantify the magnitude of mobility change in response to enforced NPIs from a network standpoint, we compute the dissimilarity between the aligned weekly networks of 2019 and 2020. To this end, we consider ego-network-based node features by Berlingerio et al. Berlingerio et al. (2012) that aim to infuse a small set of aggregated descriptive features, such as degree and clustering coefficient. In the node-level dissimilarity analysis, paired node feature vectors are utilized without any aggregation, and a score is generated for each node. Canberra distance (Lance & Williams, 1967) is applied to the paired feature vectors to quantify their dissimilarity. For further details, please see the Supplementary Information.

Centrality evolution. Neighborhoods with different demographic backgrounds manifest varying repercussions to the enforced NPIs over time, due to their distinctive needs and socioeconomic dynamics. In parallel, CBGs with ample POIs become frequent destinations. To this end, centrality metrics are employed to demonstrate the temporal change in the topological importance of the CBGs in the mobility network structure. In particular, we focus on *betweenness*, *in-degree*, *out-degree*, and *self-visit ratio*. In order to estimate the number of visits to the POIs in the home CBG, the self-visit ratio of CBG c in time step t is denoted by S_c^t and formally defined as:

$$S_c^t = \frac{W_l^t}{W_l^t + W_o^t} \quad (3)$$

In Equation (3), W_l^t is the sum of weights on self-loops (i.e., visits made by residents of CBG c to the POIs inside CBG c), and W_o^t is the sum of weights on outgoing edges (i.e., total visits made by residents of CBG c to POIs located in other CBGs) in time step t . The self-visit ratio is considered as an indicator of the locality of residents visits.

COVID-19 hotspots and bridge CBGs. The mobility per CBG is a function of multiple parameters that are heavily affected by intricate social dynamics. Because of the evident correlation between mobility and the spreading of COVID-19 infections (Chang et al. 2021, Iacus et al. 2020, Xiong et al. 2020), CBGs with higher mobility rates may cause a potential threat to restraining the disease prevalence. We refer to the CBGs that rank in the top weekly new COVID-19 cases as COVID-19 hotspots, and the CBGs that interact frequently with such hotspots as COVID-19 bridge CBGs. To detect the potential bridges, we analyze the visit frequencies among CBGs. First, we consider a two-week long time span as the incubation period for new cases to emerge (Chang et al. 2021, Iacus et al. 2020). Starting from March 2nd, 2020, when the first case in NYC was reported, we isolate the CBGs in the top weekly new cases quartile in week t , and label them as hotspots. Next, in a degree-oriented setting, we isolate the CBGs that have an outgoing edge to the previously obtained hotspot CBGs in week $t - 2$ (pre-incubation period). To determine the COVID-19 bridge CBGs, percentile-based frequency filtering is applied. To this end, we investigate CBGs with occurrence frequencies in the 75th percentile as bridges. The aim of this analysis is to find out if the bridge CBGs have special socioeconomic and demographic features and to understand why they show such mobility patterns.

Huff gravity model. The Huff gravity model (Huff, 1964) is a well-known and widely used market share estimation model that focuses on the relationship between retail stores and customer patronage by modeling it as a function of distance and store attractiveness traits such as store area. To understand the mobility patterns under varying POI densities, we employ the Huff gravity model. Equation (4) formalizes the basic version of the Huff gravity model that we use in our analyses.

$$P_{ij} = \frac{\frac{A_j^\alpha}{D_{ij}^\beta}}{\sum_{k=1}^n \frac{A_k^\alpha}{D_{ik}^\beta}} \quad (4)$$

In this equation, P_{ij} corresponds to the probability of customer i choosing POI j for shopping among all available stores in her choice set k . The exponents α and β control the weights of store area and distance respectively. Since there was a significant decline in movement activities during the COVID-19 pandemic, in order to have a reasonable amount of observations that can provide a better fit for the model, we aggregate the visits from a CBG level into a census tract level. For further details, please see the Supplementary Information.

Analytical setting. To demonstrate the impact of the COVID-19 pandemic on different socioeconomic groups, we first analyze the change in network topologies in a weekly resolution at a CBG level. To this end, we extract the node-level feature vectors summarizing the statistical properties of their respective ego-networks (Berlingerio et al. 2012). The resulting node feature vectors are then used to compute the dissimilarities between paired weekly networks from 2019 and 2020. Then, we analyze the course of centrality metrics with respect to different demographic groups and highlight their variability. Next, we analyze the possible COVID-19 bridges, neighborhoods that frequently interact with COVID-19 hotspots (CBGs with a higher rate of infected residents), by focusing on incoming and outgoing edges between CBGs over two-week periods, which is considered as the virus incubation time (Chang et al. 2021). Finally, utilizing the Huff gravity model, we simulate the change in mobility patterns in Staten Island under different hypothetical grocery store densities in order to estimate the shift in visit patterns to hotspot

CBGs that frequently appear in the top new COVID-19 cases quartile.

Results

Demographic disparities: Temporal changes in mobility networks

CBG-level dissimilarity analysis. We compute the node-level dissimilarity scores between paired weekly networks of 2019 (pre-pandemic) and 2020 (pandemic) using the extracted ego-network feature vectors. The weeks across both years are aligned to compute dissimilarity scores for each CBG. The CBGs are then ranked with respect to their dissimilarity scores at each time step (i.e., weekly). To demonstrate the differences between the CBGs with distinct behaviors, we focus on the CBGs in the top and bottom dissimilarity quartiles and create two cohorts of CBGs that frequently appear in those quartiles during the first wave of the pandemic between March and June 2020. Figure 1 shows the spatial and socioeconomic distribution of the resulting cohorts of CBGs that appear in at least 60% of the time steps in the top and bottom dissimilarity quartiles. At a threshold value of 60%, we achieve a balanced number of CBGs in each group, facilitating a more effective comparison. To demonstrate the demographic profile of each cohort, we illustrate their distribution across socioeconomic traits using quartiles, using a color scheme consistent with the spatial distribution visualization.

Among the CBGs exhibiting the most significant shifts in their mobility patterns—belonging to the top dissimilarity quartile—a predominant concentration is observed within Manhattan, the financial center of NYC. From all CBGs in this cohort, 63% of them rank in the top quartile for income, 79% in the top education quartile (share of bachelor or higher degree holders), 62% in the top white population percentage quartile, and 52% in the bottom quartile for commute time, meaning they either do not travel relatively long distances to get to their workplace or are located in areas that have greater access to fast and frequent transportation. There is no evident socioeconomic profile for the bottom dissimilarity quartile (i.e., the group of CBGs that changed their mobility patterns the least). However, the distributions in socioeconomic quartiles delineate the residents to some extent. There exists a decreasing trend from bottom to top quartiles in income, education level, and white population percentage.

Node degree and centrality metrics. Centrality metrics help us examine a node's role in the network, such as influence and information diffusion (Deville et al. 2016, Miritello et al. 2011). In this proposed mobility network, where each node represents a CBG, centrality metrics pinpoint the CBGs that stand out due to their significant influence on mass movements.

In this context, the temporal changes in centrality metrics reveal the interaction patterns between different socioeconomic communities, which consequently indicate complex mobility behaviors from a network perspective. To this end, we concentrate on fundamental node degree centrality metrics and scrutinize their evolution within specific demographic groups, namely CBGs located in the top and bottom socioeconomic quartiles. We use the node *betweenness* to illustrate a CBG's importance based on its connections and position in the network. Furthermore, we use *degree* centrality metrics to reveal the weekly incoming and outgoing visitors among CBGs. Lastly, we use a custom metric named *self-visit ratio* to represent the fraction of visits to the POIs inside the home CBG.

Betweenness: This centrality score measures how frequently a CBG appears along the shortest paths in a network and is the only node centrality metric that demonstrates a significant difference

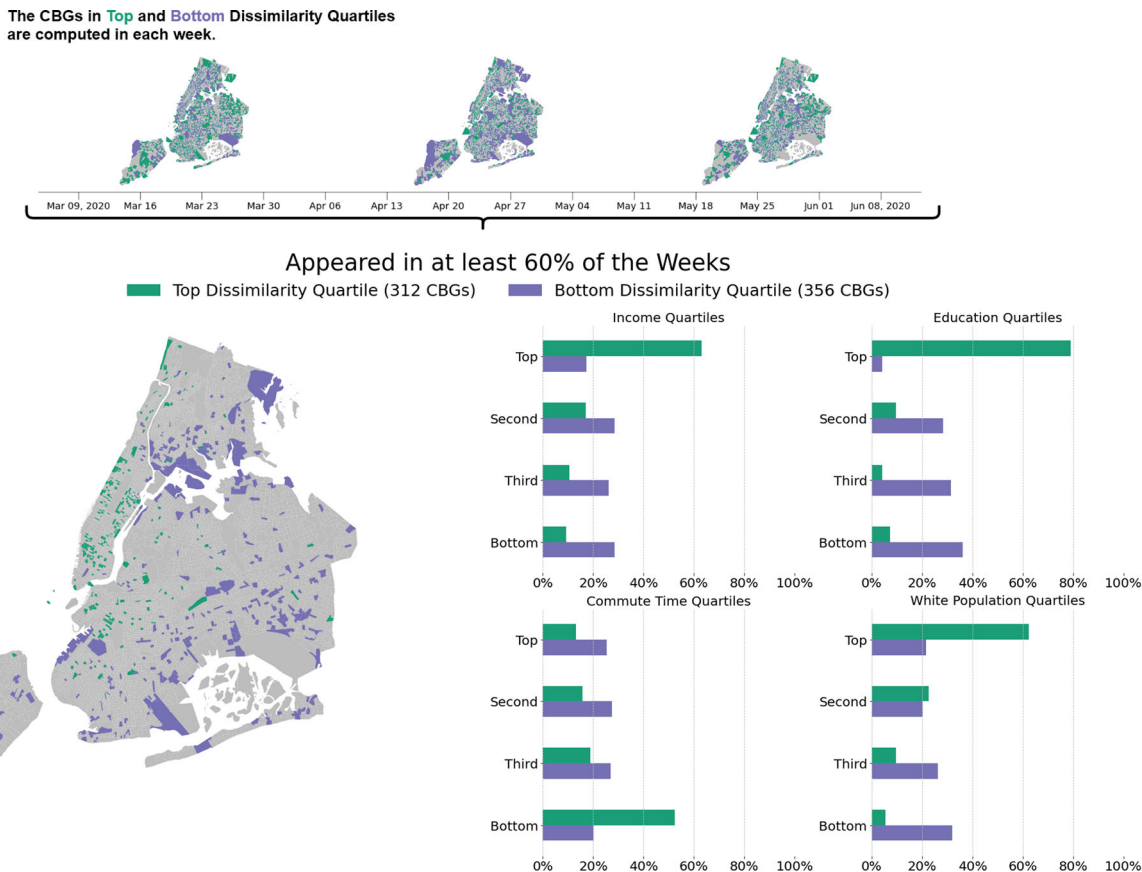


Fig. 1 The socioeconomic distribution of the CBGs that changed their mobility patterns the most, colored in green, in comparison to the previous year in at least 60% of the time steps, versus the least, colored in purple. In addition to depicting the spatial distribution, the identical coloring scheme is employed to represent the demographic characteristics of both groups, showcasing their distribution by quartiles across socioeconomic traits. Note that there are only significant socioeconomic characteristics for the top quartile CBGs but not for the bottom.

between the selected demographic groups. As displayed in Fig. 2-A, CBGs in the top income quartile held a higher betweenness value until the beginning of March 2020 (the start of the pandemic), meaning that they played a critical role in terms of bridging the flow of masses. However, an abrupt decrease of betweenness in the top-income CBGs took place after the start of the pandemic, while less affluent CBGs gained higher betweenness scores. That is, less affluent CBGs increasingly acted as connectors among the nodes in the mobility network but only until September 2020, when the economic activity revived. The same relationship can also be observed when focusing on education levels. CBGs with lower education levels had a higher betweenness score in the same time interval (Supplementary Information Figure 5).

Degree: Node degree analysis indicates that income and education play a significant role in the distribution of degree centrality values as well (Supplementary Information Figure 5). Affluent CBGs were more successful in decreasing their mobility compared to less affluent neighborhoods as shown in Fig. 2-B.

Self-Visit ratio: Another metric we defined to investigate the change in visit patterns is called the self-visit ratio. This ratio represents the proportion of visits made by residents of a particular CBG to the POIs inside their own home CBG, compared to their total number of visits (Equation (3)). Figure 2-C displays the course of the self-visit ratio with respect to the top and bottom income quartiles. From March to June 2020, during the first wave and the most striking decline in mobility, CBGs in the top-income quartile had a higher rate of visits to the POIs inside their home CBGs, while on the contrary, the residents of

lower-income CBGs displayed a lower self-visit ratio. However, starting in June 2020, as the re-opening of economic activity commenced, the disparity of self-visit ratio between income groups is narrowed.

Analysis of COVID-19 hotspots, bridge CBGs & the case of Staten Island. As explained in the Methods section, we define the COVID-19 hotspots as those CBGs that frequently appear among the CBGs with the highest weekly new COVID-19 cases. Furthermore, we designate CBGs with substantial interactions with hotspots, occurring at the onset of the virus incubation period as COVID-19 bridge CBGs. Examining the COVID-19 bridge CBGs can potentially reveal invaluable insights for policymakers and urban planners attempting to prevent the spread of new infections and build cities that are resilient to future pandemics.

To achieve this, we initially identify the hotspot CBGs by isolating the top quartile in terms of weekly new cases at each time step t . Subsequently, we compile a list of potential bridge CBGs that were connected to the hotspot CBGs in time step $t - 2$, accounting for a two-week period as the incubation time for new cases to emerge. Afterward, we apply a frequency analysis on the possible bridges to check how often they were connected to CBGs with the highest weekly cases. Finally, we list the CBGs in the 75th frequency percentiles as bridges, to be considered for further analyses.

As demonstrated in Fig. 3, the majority of the resulting CBGs in the 75th frequency percentile are comprised of those in the lower quartiles for income and education and higher quartiles for

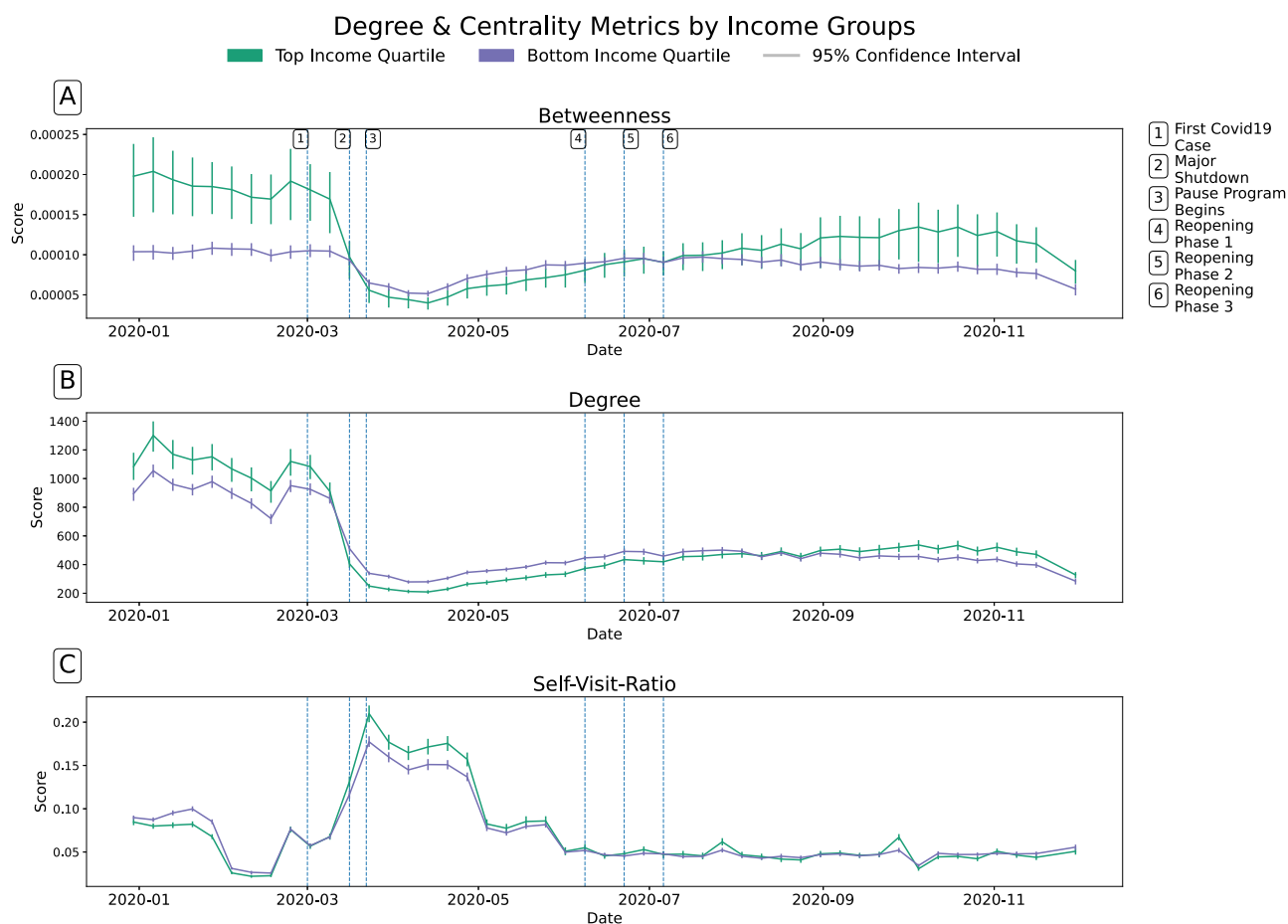


Fig. 2 The temporal change in **A** betweenness, **B** total-degree, and **C** self-visit ratio metrics in the top (green) and bottom (purple) income quartiles. Vertical dashed lines depict the milestones of the pandemic. The vertical line segments on the curves show a 95% confidence interval.

commuting time. Yet the spatial distribution of the potential bridges in the 75th frequency percentile in Fig. 3 unveils the special case of Staten Island, where 90% of the CBGs located in Staten Island are identified as the COVID-19 birdges. Moreover, as the threshold value is increased to the 95th frequency percentile, the demographic features begin to display Staten Island's presence. Figure 4 shows the box plot of the COVID-19 bridge CBGs at a borough level.

We further extend the analysis to a scenario where edge weights are incorporated, controlling for the volume of interactions based on the premise that a greater number of visits could increase the risk of virus transmission. Despite this additional consideration, our findings reveal that the outcomes are consistent whether we examine the network structures with or without weighting the edges. For more details, please see the Supplementary Information.

Subsequently, we perform an Ordinary Least Squares regression (OLS) analysis to further investigate the association between the geographic location of CBGs and their appearance in the set of the COVID-19 bridge CBGs. In the corresponding regression model, the frequency of presence among the set of bridge CBGs is the dependent variable, and borough code is the independent variable. The regression analysis results reveal the significant predictive influence of boroughs on the occurrences of CBGs within the bridge set, thus, confirming the frequency analysis results that underscored the presence of about 90% of the CBGs located in Staten Island among the COVID-19 bridge CBGs. The regression analysis results are provided in the Supplementary Information.

This study reveals a surprising pattern in the mobility behavior of CBGs in Staten Island, which is counter-intuitive and does not align with the previous findings that primarily attribute neighborhood adaptability in adhering to different NPIs to their demographic factors. Despite 48% of Staten Island's CBGs being classified in the high-income bracket with predominantly white residents - characteristics shared with CBGs in other boroughs - Staten Island exhibits unique mobility trends. This distinction is particularly striking given Staten Island's relative geographical isolation and limited connectivity to other boroughs, primarily through bridges and ferries, and its lack of direct access to the New York City subway system. Contrary to expectations, one might anticipate Staten Island to have been more insulated from the impacts of the pandemic. To better understand this anomaly, we conducted further borough-level analysis, aiming to illuminate the underlying factors driving this unexpected trend.

Borough level analyses results. Since the Safegraph mobility data has limited coverage on workplaces and offices, we use Google's COVID-19 Community Mobility Reports (goo, 2023) to investigate the mobility trends for places of work. As shown in Fig. 5, Staten Island has the minimum relative change in mobility trends for workplaces among all NYC boroughs, indicating that the residents of Staten Island reduced their mobility and visits to POIs noticeably less than the residents of other boroughs.

Additionally, the POIs analysis results show that Staten Island has the lowest number and diversity of POIs among all boroughs of NYC, where the majority of visits to POIs inside the city originating from Staten Island are made to Brooklyn and

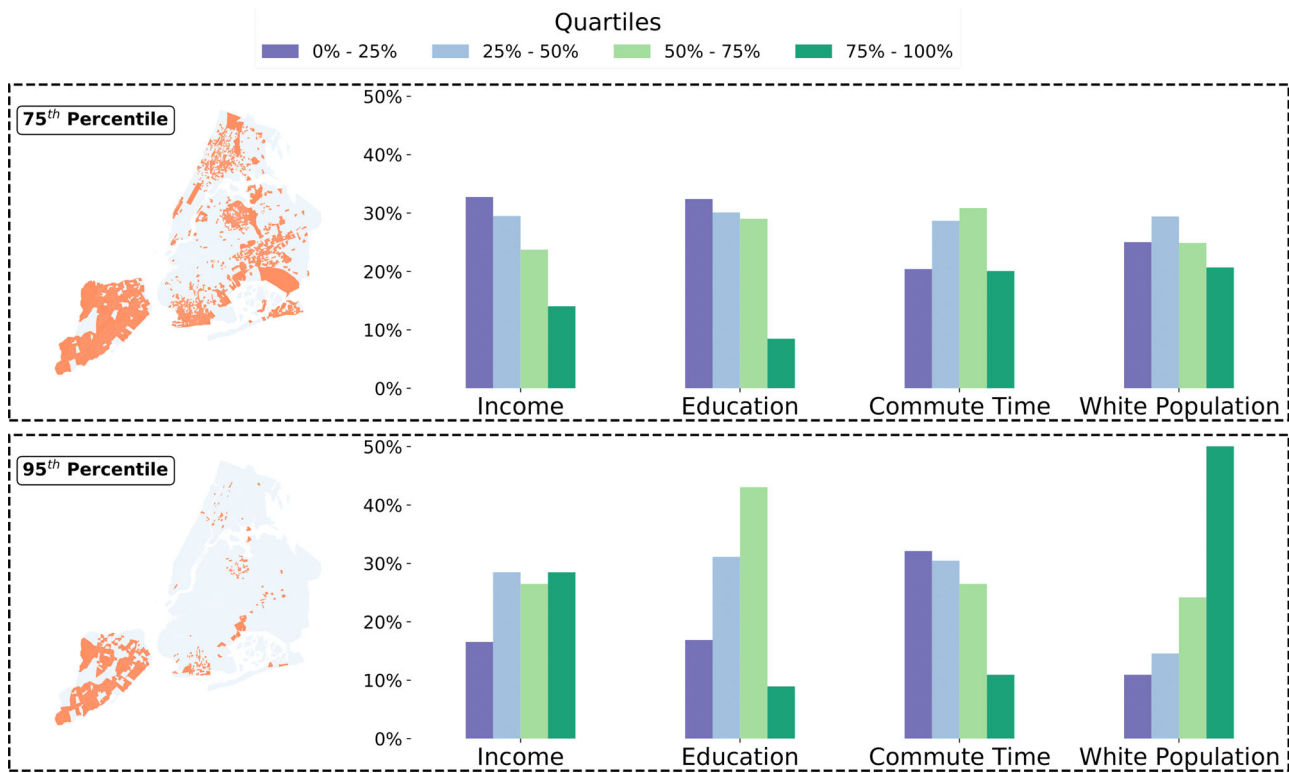


Fig. 3 The spatial and demographic distributions of CBGs within the 75th and 95th frequency percentiles, identified as COVID-19 bridges, highlight Staten Island as a distinct standout. The distributions of sociodemographic attributes are displayed by their quartiles as bar charts.

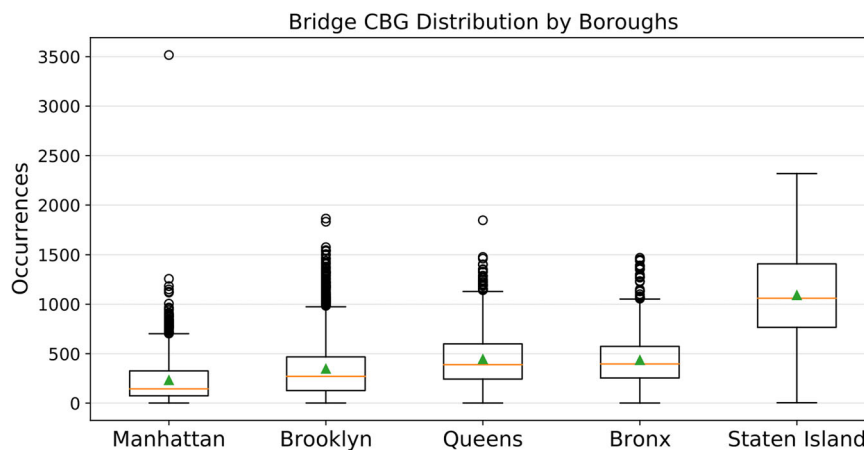


Fig. 4 A box plot demonstrating the distribution of bridge CBGs, illustrating the frequency of identification for CBGs within each borough as bridge CBGs. The y-axis shows the bridge occurrences in each borough.

Manhattan, which are the neighboring boroughs of Staten Island. This observation is in line with a report by the NYC government’s planning department (NYC Planning) documenting that 24% of workers residing in Staten Island have their workplaces located in Manhattan.

In summary, in Staten Island due to the shortage of POIs and its relatively isolated location (e.g., just one automobile bridge to Brooklyn, three automobile bridges to New Jersey, one free ferry to Manhattan, no subway), which promotes using personal cars (NYC Department of Transportation; NYC Planning), the residents had to visit POIs in other boroughs to accommodate their needs and thus traveled longer distances to workplaces and the majority of POI categories. We conclude that this is likely why we observe the CBGs in Staten Island displayed a distinct response behavior compared to their demographic counterparts

(i.e., relatively high income and high percentage of white population CBGs), and that this is what led to higher infection rates in its neighborhoods.

Hypothetical scenario analysis. In order to understand the mobility patterns of CBGs in Staten Island under hypothetical POI distributions, we perform a simulation analysis utilizing the Huff Gravity Model (Huff, 1964) that focuses on two attractiveness factors, namely: the distance between CBGs and POIs, and POI areas in square meter. More details are provided in the Supplementary Information. In addition, instead of including all POI categories, we only incorporated grocery stores into the model to narrow down the scope of our simulation analysis to those stores that provide the most essential needs of human daily

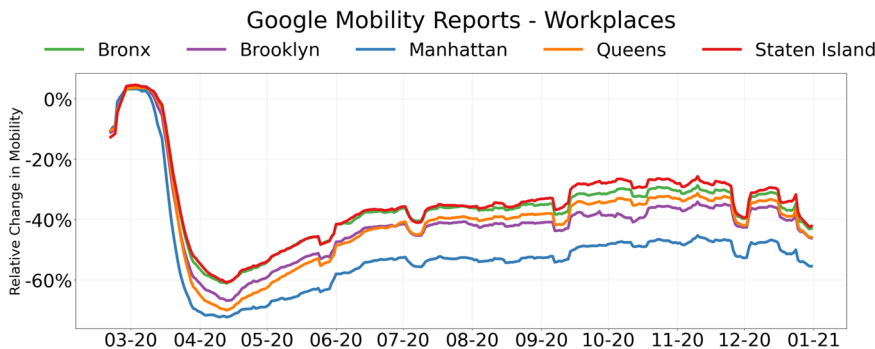


Fig. 5 Relative change in mobility trends for the workplace by borough. The x-axis displays the months-years of the focused time span while the y-axis shows the relative change in the borough-level mobility to workplaces.

Table 1 Number of grocery stores per 1,000 (1K) residents and the median distance traveled from home to grocery stores from March 22nd to June 8th, 2020, by residents of NYC boroughs.

Borough name	Grocery stores per 1K residents	Median distance traveled (in km)
Manhattan	0.582	0.90
Brooklyn	0.470	1.35
Bronx	0.435	1.26
Queens	0.414	1.71
Staten Island	0.332	2.66

life. Table 1 provides extracted information from the dataset, about the number of grocery stores per 1K residents and the median distance traveled by residents of NYC to visit grocery stores in kilometers from March 22nd to June 8th, 2020 at borough level.

As shown in Table 1, Staten Island has the lowest number of grocery stores per resident and at the same time the highest distance traveled by residents to visit a grocery store among all NYC boroughs. Our aim is to simulate the mobility patterns of Staten Island residents with a higher POI density equal to that of other boroughs with similar demographic traits. We choose the analysis time frame to be during the first wave of the pandemic between March 22nd (pause program start date) and June 8th (phase I of the reopening) of 2020. Since the NYC officials enforced a strict citywide lockdown policy during this time frame (Birge et al. 2022), most of the workplaces were closed, and only essential businesses like grocery stores were allowed to operate. Therefore, we contend that most trips to grocery stores during that time frame could be considered single-purpose trips rather than multi-purpose ones (Lucchini et al. 2021), and thus it is reasonable to use the distance between the stores and customers' home locations in the model as a proxy for the traveled distance. Moreover, due to the lowered mobility levels during the lockdown period, we use *census tract* level visit patterns to capture broader mobility observations. It is important to note that, on average, there are about 4 CBGs per census tract. We consider each census tract as an independent mobility center and develop a model based on the aggregated mobility patterns within the defined time frame. This approach allows us to estimate the probabilities or fractions of visits paid by residents of a specific census tract to the POIs of study. For more details, please refer to the Supplementary Information.

We add randomly generated hypothetical grocery stores with an area equal to the mean grocery store area within Staten Island and continue until the new grocery stores per 1K residents match the grocery store densities of Manhattan and Queens, which are

the two other boroughs with more similar demographics to that of Staten Island. We employ historical mobility data to generate the synthetic visit numbers based on the previously derived probabilities within the hypothetical scenario. Next, we accumulate the synthetic visits to the POIs located in the hotspot CBGs. We aggregate the visits in each census tract both for the ground truth and simulated cases and then analyze the change in visits by residents of Staten Island to hotspot CBGs, that frequently appear in the top new cases quartile. The simulation results show that the visits to hotspot CBGs by Staten Island residents decreased by 47% and 23% under scenarios of Manhattan and Queens' grocery store densities, respectively. Such results mean less exposure to possible COVID-19 spreaders and a lower risk of contamination that can potentially lead to a reduced mortality rate.

Discussion

In this research, we build on the tradition of using network structures to explain human behavior in socioeconomic settings by examining the complex relationship between human mobility, demographic attributes, and socioeconomic outcomes within the context of the COVID-19 pandemic. In particular, we take a network analysis approach to understanding the impact of the COVID-19 pandemic and its associated NPIs on the mobility patterns of NYC residents across its five boroughs, covering 6,493 census block groups (CBGs), throughout the year 2020. The network nodes represent CBGs, and the links correspond to visits between pairs of CBGs using visits to POIs by residents. We investigate node-specific and ego-network-based structural features to compute dissimilarity scores between weekly networks year-on-year for 2019 and 2020 to quantify the magnitude of change in the network structure.

In addition, we analyze the temporal changes in node and degree centrality measurements across different socioeconomic groups. Our findings reveal that while the COVID-19 response measures resulted in substantial changes in the mobility network structure, the CBGs that changed their ego-network structure the least had higher COVID-19 infection rates. The majority of such nodes are from low-income and low-education level neighborhoods with higher rates of front-line workers (e.g., workers in healthcare, grocery, convenience and drug stores, child care, food and family services, public transport, trucking, warehouse, and postal services) who could not reduce their mobility by as much (Office of the New York City Comptroller). Arguably this is because of their job type that requires working outside their home and keep commuting frequently.

The results of our CBG-level ego-network dissimilarity analysis suggest a clear demographic distinction of residents who live in CBGs with top-dissimilarity scores that appeared in >60% of the weekly patterns we analyzed: high-income, higher education level, and mostly white population. We contend that these are residents

whose job types can most suitably respond to the shelter-in-place and physical/social distancing orders through remote work, unlike the residents in neighborhoods with other job types. Hence, in alignment with other studies (Chang et al. 2021, Chetty et al. 2020, Hunter et al. 2021), our findings indicate that the residents of CBGs with top dissimilarity scores, demonstrate greater resilience during pandemics like COVID-19. They are better equipped to adapt to NPIs that necessitate restricted mobility.

Two-sides of the same city. Using a network perspective, we extend the previous work by finding that the adaptability of mobility patterns varies significantly among communities not only by their socioeconomic and demographic features but also by geographical attributes of their neighborhoods. Quantifying the year-on-year weekly ego-network dissimilarities, we show that the less affluent and less educated neighborhoods demonstrated less adaptability to policy interventions aimed at reducing their mobility level. In addition, as a major contribution of this study, we show that the residents of neighborhoods with higher income and higher education levels can demonstrate similar behavior to less affluent and less educated neighborhoods if they have relatively limited access to public transport, workplaces, shops, and a set of other diverse amenities, as is the case with Staten Island.

Despite the limited physical connections between Staten Island and other boroughs of NYC and New Jersey, which might suggest a breakdown of the existing mobility network in the face of an extreme exogenous shock, our findings reveal a contrasting scenario. Contrary to expectations, the changes observed in the network structure were surprisingly minimal. Therefore, Staten Island was relatively fragile to the COVID-19 pandemic in terms of infections. Exploring similar neighborhoods or isolated geographical blocks in other urban areas could be the subject of future research to help policy-makers develop effective policies to alleviate the burden of a pandemic in such areas and increase their resilience and adaptability to public health interventions that necessitate reduced mobility.

Opportunities for urban planning. Our study provides valuable insights for urban planning and offers significant contributions to policy development. It underscores the importance of integrating both socioeconomic and geographic dimensions and characteristics of neighborhoods, including their physical structures, in efforts to enhance resilience against future external shocks. Specifically, this involves enhancing the adaptability of neighborhoods to potential interventions proposed by experts and authorities. Our findings highlight the necessity of a holistic approach to urban development, one that recognizes and addresses the diverse attributes of communities for more effective and sustainable resilience-building strategies.

With regards to the latter and based on our simulation results, convenient access to POIs that provide daily essential needs (e.g., grocery stores), workplaces, and centers of attraction that offer a variety of amenities through a diverse set of POIs would be expected to reduce the need for traveling long distances. Using a Huff Gravity Model we performed a hypothetical scenario analysis to estimate the number of visits to COVID-19 hotspot CBGs with hypothetically added grocery stores for each CBG in Staten Island. Although we only consider customer-store distance and POI floor area in our model, the results yield valuable insights regarding simulated mobility. Our findings indicate that as a result of the increase in access to essential POIs, residents are less exposed to the COVID-19 hotspot CBGs and are able to satisfy their needs without traveling further distances. In cases like the COVID-19 pandemic, an increased level of access to

POIs, could potentially decrease the level of infections and save more lives.

As the continued pandemic conditions reveal, these factors might be a major influence on future work habits and trends, and resilient communities organized and structured along these lines might be the preferred choice for many members of the population. As a future research direction, we aim to extend our simulation analysis by incorporating more POI categories with additional POI attractiveness features and other relevant attributes such as a neighborhood's physical characteristics into the model to evaluate the results within different settings. Furthermore, we are also planning to extend our current mobility analysis by illustrating the effects of hypothetical grocery stores using flow graphs between urban areas such as boroughs.

Limitations. Our study encounters certain constraints primarily due to the nature of the datasets used. The mobility trends and visits to POIs are aggregated on a time-based (e.g., weekly) and neighborhood-level (e.g., CBGs) framework. While this approach effectively safeguards the privacy of smartphone users (Bahrami, 2023), it consequently limits our ability to capture the specific motivations behind users' trips to various destination CBGs (e.g., for work, shopping, entertainment, or other purposes). This additional level of detail would allow us to distinguish between essential and non-essential trips made by residents and match them with the socioeconomic characteristics of neighborhoods.

Originating from the same limitation, we are only able to see which neighborhoods are connected to one another in the form of visits and with what frequency, but not how (i.e., mode of transportation) they are connected. Although it may be possible to infer the predominant transportation modes and routes between CBGs using alternative and additional datasets, the resolution of our data is insufficient for correlating these with individual trips. Consequently, this precludes further examination into the proportion of trips conducted via various modes of transportation, and how these relate to virus transmission and community resilience.

Furthermore, the POI dataset we use in our study mostly includes places where financial transactions take place (e.g., supermarkets, dentist offices, restaurants) and has a low coverage of workplaces and offices (e.g., corporate buildings, co-work spaces). The latter could help us identify additional types of essential travels (e.g., workplace commutes) and better fit the gravity model for simulation purposes. We tried to address this limitation partially by using complementary datasets such as Google's mobility report and the mobility survey results published by NYC city officials.

The findings derived from the hypothetical scenario analysis indicate that increased accessibility to essential amenities plays a significant role in reducing infection rates. However, such a scenario relies on private developers to provide essential services and POIs like grocery stores, workplaces, and attractive amenities in potentially economically disadvantaged neighborhoods. Therefore, a limitation can arise from the utopian recommendation of opening additional and in some cases excessive essential businesses in the areas that are not financially attractive for the private sector. To address this issue, there are several approaches, including government policies like tax exemption zones designed to encourage private sector involvement in commercial activities. Nonetheless, the primary objective of our study is to straightforwardly assess various hypothetical scenarios, with a particular emphasis on estimating the scale of their impact on the mobility patterns of residents.

Finally, despite all the limitations, our study makes at least two major contributions. First, our study results contribute

substantive insights into the heterogeneity of mobility patterns among different neighborhoods during the COVID-19 pandemic through leveraging network science approaches and quantitative scenario analysis. Second, our study illuminates the factors associated with a neighborhood's resilience and fragility. Understanding the factors associated with a neighborhood's resilience and fragility can help urban planners and authorities recommend sustainable policies, make better intervention decisions, and be prepared to react more effectively to future exogenous shocks like the COVID-19 pandemic and save more lives.

Data availability

All the datasets and scripts used for this study are available for further research and replication purposes. The Safegraph mobility dataset is available for academic research purposes through request at: <https://www.safegraph.com/>. The Google COVID-19 Community Mobility Reports data is available at: <https://www.google.com/covid19/mobility/>. All scripts are available at the project GitHub repository: <https://github.com/hasanalpboz/safegraph-covid19-mobility>

Received: 27 July 2023; Accepted: 26 February 2024;

Published online: 12 March 2024

References

- Google (2023) COVID-19 community mobility reports. Available online at: <https://www.google.com/covid19/mobility/>. Accessed on 23 November 2023
- Aleta A, Martin-Corral D, Piontti APY, Ajelli M, Litvinova M, Chinazzi M, Dean NE, Halloran ME, Longini Jr IM, Merler S et al. (2020) Modelling the impact of testing, contact tracing and household quarantine on second waves of COVID-19. *Nature Human Behaviour* 4(9):964–971
- Althouse BM, Wallace B, Case, B, Scarpino SV, Allard A, Berdahl AM, White ER and Hébert-Dufresne L (2020) The unintended consequences of inconsistent pandemic control policies. *medRxiv* <https://doi.org/10.1101/2020.08.21.20179473>
- Alvarez FE, Buera FJ, Lucas RE et al. (2013) Idea flows, economic growth, and trade. *NBER* <https://doi.org/10.3386/w19667>
- Badr HS, Zaitchik BF, Kerr GH, Nguyen N-LH, Chen Y-T, Hinson P, Colston JM, Kosek MN, Dong E, Du H et al. (2023) Unified real-time environmental-epidemiological data for multiscale modeling of the covid-19 pandemic. *Sci Data* 10(1):367
- Bahrami MA (2023) A perspective towards using aggregated D\data in research. *OSF* <https://doi.org/10.31219/osf.io/k268q>
- Bahrami M, Boz HA, Suhara Y, Balcisoy S, Bozkaya B, Pentland A (2023) Predicting merchant future performance using privacy-safe network-based features. *Sci Rep* 13(1):10073
- Berlingerio M, Koutra D, Eliassi-Rad T, Faloutsos, C (2012) Netsimile: A scalable approach to size-independent network similarity. *arXiv* <https://doi.org/10.48550/arXiv.1209.2684> (2012)
- Bettencourt LM (2013) The origins of scaling in cities. *Science* 340(6139):1438–1441
- Bettencourt LM, Lobo J, Helbing D, Kühnert C, West GB (2007) Growth, innovation, scaling, and the pace of life in cities. *Proc Natl Acad Sci USA* 104(17):7301–7306
- Birge JR, Candogan O, Feng Y (2022) Controlling epidemic spread: reducing economic losses with targeted closures. *Manag Sci* 68(5):3175–3195
- Buera FJ, Oberfield E (2020) The global diffusion of ideas. *Econometrica* 88(1):83–114
- Chang S, Pierson E, Koh PW, Gerard J, Redbird B, Grusky D, Leskovec J (2021) Mobility network models of covid-19 explain inequities and inform reopening. *Nature* 589(7840):82–87
- Chang S, Vrabac D, Leskovec J, Ugander J (2023) Estimating geographic spillover effects of covid-19 policies from large-scale mobility networks. *Proc AAAI Conf Artif Intell* 37:14161–14169
- Chetty R, Friedman JN, Hendren N, Stepner M and Opportunity Insights Team (2020) The economic impacts of COVID-19: Evidence from a new public database built using private sector data. *Q J Econ* <https://doi.org/10.1093/qje/qjad048>
- Chong SK, Bahrami M, Chen H, Balcisoy S, Bozkaya B et al. (2020) Economic outcomes predicted by diversity in cities. *EPJ Data Sci.* 9(1):17
- Deville P, Song C, Eagle N, Blondel VD, Barabási A-L, Wang D (2016) Scaling identity connects human mobility and social interactions. *Proc Natl Acad Sci USA* 113(26):7047–7052
- Edsberg Møllgaard P, Lehmann S, Alessandretti L (2022) Understanding components of mobility during the covid-19 pandemic. *Philos Trans R Soc A* 380(2214):20210118
- Fan C, Lee R, Yang Y, Mostafavi A (2021) Fine-grained data reveal segregated mobility networks and opportunities for local containment of covid-19. *Sci Rep* 11(1):16895
- Flaxman S, Mishra S, Gandy A, Unwin HJT, Mellan TA, Coupland H, Whittaker C, Zhu H, Berah T, Eaton JW et al. (2020) Estimating the effects of non-pharmaceutical interventions on COVID-19 in Europe. *Nature* 584(7820):257–261
- Galeazzi A, Cinelli M, Bonaccorsi G, Pierri F, Schmidt AL, Scala A, Pammolli F, Quattrociocchi W (2021) Human mobility in response to covid-19 in France, Italy and UK. *Sci Rep* 11(1):13141
- Garcia-Bulle B, Horn AL, Bell BM, Bahrami M, Bozkaya B, Pentland A, de la Haye K Moro E (2022) You are where you eat: effect of mobile food environments on fast food visits. *medRxiv* <https://doi.org/10.1101/2022.09.20.22280128>
- Gauvin L, Bajardi P, Pepe E, Lake B, Privitera F, Tizzoni M (2021) Socio-economic determinants of mobility responses during the first wave of covid-19 in italy: from provinces to neighbourhoods. *J R Soc Interface* 18(181):20210092
- Heroy S, Loaiza I, Pentland A, O'Clery N (2021) Covid-19 policy analysis: labour structure dictates lockdown mobility behaviour. *J R Soc Interface* 18(176):20201035
- Horn AL, Bell BM, Bueno BGB, Bahrami M, Bozkaya B, Cui Y, Wilson JP, Pentland A, Moro E, de la Haye K (2021) Investigating mobility-based fast food outlet visits as indicators of dietary intake and diet-related disease. *medRxiv* <https://doi.org/10.1101/2021.10.28.21265634>
- Huff DL (1964) Defining and estimating a trading area. *J Mark* 28(3):34–38
- Hunter RF, Garcia L, de Sa TH, Zapata-Diomed B, Millett C, Woodcock J, Pentland A, Moro E (2021) Effect of covid-19 response policies on walking behavior in us cities. *Nat Commun* 12(1):1–9
- Iacus SM, Santamaria C, Sermi F, Spyrtatos S, Tarchi D, Vespe M (2020) Human mobility and covid-19 initial dynamics. *Nonlinear Dyn* 101(3):1901–1919
- Kraemer MUG, Yang C-H, Gutierrez B, Wu C-H, Klein B, Pigott DM, O. C.-. D. W. Group, du Plessis L, Faria NR, Li R, Hanage WP, Brownstein JS, Layan M, Vespignani A, Tian H, Dye C, Pybus OG, Scarpino SV (2020) The effect of human mobility and control measures on the covid-19 epidemic in china. *Science* 368(6490):493–497
- Lance GN, Williams WT (1967) Mixed-data classificatory programs i—agglomerative systems. *Aust Comput J* 1(1):15–20
- Lazer D, Pentland A, Adamic L, Aral S, Barabási A-L, Brewer D, Christakis N, Contractor N, Fowler J, Gutmann M, Jebara T, King G, Macy M, Roy D, Alstey MV (2009) Computational social science. *Science* 323(5915):721–723
- Lucchini L, Centellegher S, Pappalardo L, Gallotti R, Privitera F, Lepri B, De Nadai M (2021) Living in a pandemic: changes in mobility routines, social activity and adherence to covid-19 protective measures. *Sci Rep* 11(1):1–12
- Miritello G, Moro E, Lara R (2011) Dynamical strength of social ties in information spreading. *Phy Rev E* 83(4):045102
- NYC Department of Transportation (2023) NewYork City Mobility Report 2019. Available online at: <http://www.nyc.gov/html/dot/downloads/pdf/mobility-report-2019-print.pdf>. Accessed on 23 November 2023
- NYC Planning (2023) The ins and outs of NYC commuting. Available online at: <https://www1.nyc.gov/assets/planning/download/pdf/planning-level/housing-economy/nyc-ins-and-out-of-commuting.pdf>. Accessed on 23 November 2023
- Office of the New York City Comptroller (2023) NewYork City's frontline workers. Available online at: <https://comptroller.nyc.gov/reports/new-york-citys-frontline-workers/>. Accessed on 23 November 2023
- Pan W, Ghoshal G, Krumme C, Cebrian M, Pentland A (2013) Urban characteristics attributable to density-driven tie formation. *Nat Commun* 4(1):1–7
- SafeGraph (2023) Weekly patterns. Available online at: <https://docs.safegraph.com/docs/weekly-patterns>. Accessed on 23 November 2023
- Schlöpfer M, Dong L, O'Keefe K, Santi P, Szell M, Salat H, Anklesaria S, Vazifeh M, Ratti C, West GB (2021) The universal visitation law of human mobility. *Nature* 593(7860):522–527
- Schlosser F, Maier BF, Jack O, Hinrichs D, Zachariae A, Brockmann D (2020) Covid-19 lockdown induces disease-mitigating structural changes in mobility networks. *Proc Natl Acad Sci USA* 117(52):32883–32890
- Singh VK, Bozkaya B, Pentland A (2015) Money walks: implicit mobility behavior and financial well-being. *PloS One* 10(8):e0136628
- Statista (2023) GDP of the New York metro area from 2001 to 2020. Available online at: <https://www.statista.com/statistics/183815/gdp-of-the-new-york-metro-area/>. Accessed on 23 November 2023
- Steele JE, Sundsøy PR, Pezzulo C, Alegana VA, Bird TJ, Blumenstock J, Bjelland J, Engo-Monsen K, de Montjoye Y-A, Iqbal AM et al. (2017) Mapping poverty using mobile phone and satellite data. *J R Soc Interface* 14(127):20160690
- Sveikauskas L (1975) The productivity of cities. *Q J Econ* 89(3):393–413
- Xiong C, Hu S, Yang M, Luo W, Zhang L (2020) Mobile device data reveal the dynamics in a positive relationship between human mobility and covid-19 infections. *Proc Natl Acad Sci USA* 117(44):27087–27089

Yabe T, Bueno BGB, Frank M, Pentland A, Moro E (2023) Behavior-based dependency networks between places shape urban economic resilience. arXiv <https://doi.org/10.48550/arXiv.2311.18108>

Yuan Y, Jahani E, Zhao S, Ahn Y-Y, Pentland AS (2023) Implications of covid-19 vaccination heterogeneity in mobility networks. *Commun Phy* 6(1):206

Author contributions

The initial idea for the research was conceptualized by HAB, MB, NM, SB, BB, and AP. The research was developed and designed by HAB, MB, NM, SB, AN, and BB. HAB and MB prepared and analyzed the data. AP and SB supervised the work. The first draft was written by HAB and MB, and later edited by HAB, MB, NM, SB, AN, and BB. The final version was approved by all authors.

Competing interests

The authors declare no competing interests.

Ethical approval

This article does not contain any studies with human participants performed by any of the authors.

Informed consent

This article does not contain any studies with human participants performed by any of the authors.

Additional information

Supplementary information The online version contains supplementary material available at <https://doi.org/10.1057/s41599-024-02881-1>.

Correspondence and requests for materials should be addressed to Hasan Alp Boz or Mohsen Bahrami.

Reprints and permission information is available at <http://www.nature.com/reprints>

Publisher's note Springer Nature remains neutral with regard to jurisdictional claims in published maps and institutional affiliations.



Open Access This article is licensed under a Creative Commons Attribution 4.0 International License, which permits use, sharing, adaptation, distribution and reproduction in any medium or format, as long as you give appropriate credit to the original author(s) and the source, provide a link to the Creative Commons licence, and indicate if changes were made. The images or other third party material in this article are included in the article's Creative Commons licence, unless indicated otherwise in a credit line to the material. If material is not included in the article's Creative Commons licence and your intended use is not permitted by statutory regulation or exceeds the permitted use, you will need to obtain permission directly from the copyright holder. To view a copy of this licence, visit <http://creativecommons.org/licenses/by/4.0/>.

© The Author(s) 2024